

GAMMA-RAY BURST EARLY OPTICAL AFTERGLOWS: IMPLICATIONS FOR THE INITIAL LORENTZ FACTOR AND THE CENTRAL ENGINE

BING ZHANG¹, SHIHO KOBAYASHI^{1,2}, & PETER MÉSZÁROS^{1,2}

¹Department of Astronomy & Astrophysics, Pennsylvania State University, University Park, PA 16802

²Department of Physics, Pennsylvania State University, University Park, PA 16802

Draft version October 21, 2019

ABSTRACT

Early optical afterglows have been observed from GRB 990123, GRB 021004, and GRB 021211, which reveal rich emission features attributed to reverse shocks. It is expected that *Swift* will discover many more early afterglows. Here we introduce a straightforward recipe for directly constraining the initial Lorentz factor of the fireball using the combined forward and reverse shock optical afterglow data. The scheme is largely independent of the shock microphysics. We identify two types of combinations of the reverse and forward shock emission, and explore their parameter regimes. We also discuss a possible diagnostic for magnetized ejecta.

Subject headings: gamma rays: bursts - shock waves

1. INTRODUCTION

The standard Gamma-ray burst (GRB) afterglow model (Mészáros & Rees 1997a; Sari, Piran & Narayan 1998) invokes synchrotron emission of electrons from the forward external shock, and has been proven successful in interpreting the late time broadband afterglows. At these late times the fireball is already decelerated and has entered a self-similar regime, in which precious information about the early ultra-relativistic phase is lost. In the very early afterglow epoch, the emission from the reverse shock propagating into the fireball itself also plays a noticeable role, especially in the low frequency bands, e.g. optical or radio (Mészáros & Rees 1997a; Sari & Piran 1999b), and information about the fireball initial Lorentz factor could be in principle retrieved from the reverse shock data. For a long time, evidence for reverse shock emission was available only from GRB 990123 (Akerlof et al. 1999; Sari & Piran 1999a; Mészáros & Rees 1999; Kobayashi & Sari 2000). Recently, thanks to prompt localizations of GRBs by the *High Energy Transient Explorer 2* (*HETE-2*) (e.g. Shirasaki et al. 2002; Crew et al. 2002) and rapid follow-ups by robotic optical telescopes (e.g. Fox 2002; Li et al. 2002; Fox & Price 2002; Park et al. 2002; Wolzniak et al. 2002), reverse shock emission has also been identified from GRB 021211 (Fox et al. 2003; Li et al. 2003; Wei 2003) and possibly also from GRB 021004 (Kobayashi & Zhang 2003, hereafter KZ03). It is expected that the *Swift* mission will record many GRB early optical afterglows after its launch scheduled in December 2003, which will unveil a rich phenomenology of early afterglows.

Here we propose a paradigm to analyze the early optical afterglow data, starting from tens of seconds after the gamma-ray trigger. By combining the emission information from both the forward and the reverse shocks, we discuss a way to derive or constrain the initial Lorentz factor of the fireball directly from the observables. The method does not depend on the absolute values of the poorly-known shock microphysics (e.g. the equipartition parameters ϵ_e and ϵ_B). We also categorize the early optical afterglows into two types and discuss the parameter regimes for both cases.

2. FORWARD AND REVERSE SHOCK COMPARISON

We consider a relativistic shell (fireball ejecta) with an isotropic equivalent energy E and an initial Lorentz factor γ_0 expanding into a homogeneous interstellar medium with particle number density n at a redshift z . In the observer's frame, one can define a timescale when the accumulated ISM mass is $1/\gamma_0$ of the ejecta mass, i.e., $t_\gamma = [(3E/4\pi\gamma_0^2 nm_p c^2)^{1/3}/2\gamma_0^2 c](1+z)$. This is the fireball deceleration time if the burst duration $T < t_\gamma$. For $T > t_\gamma$, the deceleration time is delayed to T . The critical condition $T = t_\gamma$ defines a critical initial Lorentz factor

$$\gamma_c \simeq 125 E_{52}^{1/8} n^{-1/8} T_2^{-3/8} [(1+z)/2]^{3/8}, \quad (1)$$

where the convention $Q = 10^n Q_n$ is used. Notice that γ_c depends on E , T , z , and n (eq.[1]), which could be either directly measured by *Swift*, or be inferred from broadband afterglow fitting (e.g. Panaiteescu & Kumar 2001), so that γ_c is essentially an observable in an idealized observational campaign. Notice also that γ_c is insensitive to the inaccuracy of measuring n and E . Generally, one can define $\gamma_0 < \gamma_c$ as the thin-shell case, while $\gamma_0 > \gamma_c$ as the thick-shell case. When the reverse shock crosses the shell, the observer time and the ejecta Lorentz factor are (Sari & Piran 1995; Kobayashi, Piran & Sari 1999)

$$t_\times = \max(t_\gamma, T), \gamma_\times = \min(\gamma_0, \gamma_c), \quad (2)$$

where the first and second values in the above expressions correspond to the thin and thick shell cases, respectively. The forward shock synchrotron spectrum can be approximated as a four-segment power-law with breaks at the cooling frequency ν_c , typical frequency ν_m and the self-absorption frequency ν_a (Sari et al. 1998), and so is the reverse shock emission spectrum at $t < t_\times$. For $t > t_\times$, there is essentially no emission above ν_c for the reverse shock emission. For both shocks, the typical frequency, cooling frequency and the peak flux scale as $\nu_m \propto \gamma B \gamma_e^2$, $\nu_c \propto \gamma^{-1} B^{-3} t^{-2}$, and $F_{\nu, m} \propto \gamma B N_e$, where γ is the bulk Lorentz boost, B is the comoving magnetic field, γ_e is the typical electron Lorentz factor in the shock-heated region,

and N_e is the total number of emitting electrons. At the shock crossing time, one has the relations (KZ03, but with a \mathcal{R}_B dependence added here)

$$\frac{\nu_{m,r}(t_x)}{\nu_{m,f}(t_x)} \sim \hat{\gamma}^{-2} \mathcal{R}_B \quad (3)$$

$$\frac{\nu_{c,r}(t_x)}{\nu_{c,f}(t_x)} \sim \mathcal{R}_B^{-3}, \quad (4)$$

$$\frac{F_{\nu,m,r}(t_x)}{F_{\nu,m,f}(t_x)} \sim \hat{\gamma} \mathcal{R}_B \quad (5)$$

where

$$\begin{aligned} \hat{\gamma} &\equiv \gamma_x^2 / \gamma_0 = \min(\gamma_0, \gamma_c^2 / \gamma_0) \leq \gamma_c, \\ \mathcal{R}_B &\equiv B_r / B_f = (\epsilon_{B,r} / \epsilon_{B,f})^{1/2} \end{aligned} \quad (6)$$

and the subscripts ‘f’ and ‘r’ indicate forward and reverse shock, respectively. In some central engine models (e.g. Usov 1992; Mészáros & Rees 1997b), the fireball wind may be endowed with “primordial” magnetic fields, so that in principle B_r could be higher than B_f , and we have included the \mathcal{R}_B parameter in a more general discussion. The forward shock emission is likely to be in the “fast cooling” regime ($\nu_{c,f} < \nu_{m,f}$) initially and in the “slow cooling” regime ($\nu_{c,f} > \nu_{m,f}$) at later times (Sari et al. 1998). For the reverse shock emission, it can be deduced from eqs. (3, 4) and eq.(11) of Sari et al. (1998) that slow cooling ($\nu_{c,r} > \nu_{m,r}$) is generally valid as long as \mathcal{R}_B is not much greater than unity.

The lightcurves can be derived by specifying the temporal evolution of ν_m , ν_c , and $F_{\nu,m}$. To first order, in the forward shock (Mészáros & Rees 1997a) we have

$$\nu_{m,f} \propto t^{-3/2}, F_{\nu,m,f} \propto t^0 \quad (7)$$

while in the reverse shock for $t > t_x$ (Kobayashi 2000, hereafter K00) we have approximately

$$\nu_{m,r} \propto t^{-3/2}, F_{\nu,m,r} \propto t^{-1} \quad (8)$$

The optical-band lightcurve for the forward shock is well-described by the “low-frequency” case of Sari et al. (1998, their Fig.2b), characterized by a turnover of the temporal indices from $1/2$ to ~ -1 at the peak time $t_{p,f}$ (at which $\nu_{m,f}$ crosses the observational band, e.g. the typical R-band frequency ν_R). The optical lightcurve for the reverse shock emission is more complicated, depending on whether the shell is thin or thick, whether it is in the slow or fast cooling regime, and how ν_R compares with $\nu_{m,r}(t_x)$ and $\nu_{c,r}(t_x)$ (see K00 for a complete discussion). For reasonable parameters, however, the cases of $\nu_R > \nu_{c,r}$ and $\nu_R < \nu_{a,r}$ are unlikely, and even if these conditions are satisfied, they do not produce interesting reverse shock signatures. Defining

$$\mathcal{R}_\nu \equiv \frac{\nu_R}{\nu_{m,r}(t_x)}, \quad (9)$$

and specifying the slow-cooling case (which is reasonable for a large sector of parameter regimes, K00), the reverse

shock lightcurves are then categorized into four cases with various temporal indices α (where $F \propto t^{-\alpha}$) separated by various break times. The four cases with their typical temporal power-law indices (in parentheses), which correspond to the thick and thin solid lines in Fig.2a and Fig.3a of K00, are: (i) thin shell $\mathcal{R}_\nu > 1$: $\sim (5, -2)$; (ii) thin shell $\mathcal{R}_\nu < 1$: $\sim (5, -1/2, -2)$; (iii) thick shell $\mathcal{R}_\nu > 1$: $\sim (1/2, -2)$; (iv) thick shell $\mathcal{R}_\nu < 1$: $\sim (1/2, -1/2, -2)$. We note that in all four cases, the final temporal power-law index is ~ -2 , corresponding to adiabatic cooling of the already accelerated electrons at t_x , with $\nu_R > \nu_{m,r}$. Strictly speaking, by writing the final lightcurve as $\propto t^{-\alpha}$, one has (eq.[8] used)

$$\alpha = (3p + 1)/4, \quad (10)$$

where p is the power law index of the electrons in the reverse shock region. We can see that $\alpha \sim 2$ for typical p values. Going backwards in time, this well-known $F_{\nu,r} \propto t^{-2}$ reverse shock lightcurve ends at t_x for $\mathcal{R}_\nu > 1$ (with a rising lightcurve before that), but at the time when $\nu_{m,r}$ crosses ν_R for $\mathcal{R}_\nu < 1$ (with a flatter declining lightcurve, $F_{\nu,r} \propto t^{-1/2}$, before) (Fig.1)¹.

We define as $t_{p,r}$ the time when the $F_{\nu,r} \propto t^{-2}$ lightcurve starts and define the corresponding reverse shock spectral flux as $F_{\nu,p,r}$ (Fig.1). The lightcurve point $(t_{p,r}, F_{\nu,p,r})$ is generally called the reverse shock peak, but strictly this is valid only when $\mathcal{R}_\nu > 1$ (in which case $t_{p,r} = t_x$). For the forward shock emission, it is natural to define the forward shock peak at $(t_{p,f}, F_{\nu,p,f})$ (Fig.1), where $F_{\nu,p,f} = F_{\nu,m,f}$ (eq.[7]). For practical purposes, it is illustrative to derive the ratio of the two peak times and that of the two peak fluxes by making use of eqs. (3), (5), (7), (8) and (10), i.e.

$$\mathcal{R}_t \equiv \frac{t_{p,f}}{t_{p,r}} = \begin{cases} \hat{\gamma}^{4/3} \mathcal{R}_B^{-2/3} \mathcal{R}_\nu^{-2/3}, & \mathcal{R}_\nu > 1, \\ \hat{\gamma}^{4/3} \mathcal{R}_B^{-2/3}, & \mathcal{R}_\nu < 1, \end{cases} \quad (11)$$

$$\mathcal{R}_F \equiv \frac{F_{\nu,p,r}}{F_{\nu,p,f}} = \begin{cases} \hat{\gamma} \mathcal{R}_B \mathcal{R}_\nu^{-2(\alpha-1)/3}, & \mathcal{R}_\nu > 1, \\ \hat{\gamma} \mathcal{R}_B \mathcal{R}_\nu^{2/3}, & \mathcal{R}_\nu < 1. \end{cases} \quad (12)$$

Notice that we have intentionally defined both \mathcal{R}_t and \mathcal{R}_F to be (usually) larger than unity, and that these expressions are valid regardless of whether the shell is thin or thick. We have assumed that both the forward and reverse-shocked regions have a same ϵ_e and p , but with different ϵ_B ’s (as parameterized by \mathcal{R}_B). Since the synchrotron emission typical frequencies and the peak flux depend on these microphysics parameters in a similar way, these parameters largely cancel out (except for \mathcal{R}_B) in eqs.(11) and (12) where we deal with the relative emission properties of the forward vs. reverse shock emissions.

3. A RECIPE TO CONSTRAIN INITIAL LORENTZ FACTOR

Reverse shock emission data have been used to estimate the initial Lorentz factor of GRB 990123 (Sari & Piran 1999a; Kobayashi & Sari 2000; Wang, Dai & Lu 2000; Soderberg & Ramirez-Ruiz 2002; Fan et al. 2002), but poorly-known shock microphysics parameters (e.g., ϵ_e , ϵ_B , p , etc.) were used in these methods. Here we introduce a

¹With eqs.(2), (3), (9), and eq.(1) of KZ03, we can derive $\mathcal{R}_\nu \sim 500 \mathcal{R}_B^{-1} \gamma_{0,2}^{-2} n^{-1/2} \epsilon_{B,-2}^{-1/2} \epsilon_{e,-1}^{-2} [g/(1/3)]^{-2} [(1+z)/2]$, where $g = (p-2)/(p-1)$. We can see that generally $\mathcal{R}_\nu > 1$, but the $\mathcal{R}_\nu \lesssim 1$ case is also allowed for some extreme parameters.

simple method to do so with the shock microphysics parameters largely canceled out.

We first consider an “idealized” observational campaign, which may be realized with *Swift* or a similar facility. We assume that the optical lightcurve is monitored starting early enough that both the reverse and forward shock “peaks”, i.e., $(t_{p,r}, F_{\nu,p,r})$ and $(t_{p,f}, F_{\nu,p,f})$ are identified, and that the fast-decaying reverse shock lightcurve index α is measured. As a result, \mathcal{R}_t , \mathcal{R}_F and α are all known parameters. Notice that since both peaks are essential for our method, *we strongly recommend that the Swift UVOT instrument closely follow a GRB early lightcurve until the forward shock peak is identified*. With eqs.(11) and (12), we can directly solve for $\hat{\gamma}$ and \mathcal{R}_ν for two \mathcal{R}_ν regimes, in terms of \mathcal{R}_t , \mathcal{R}_F and α , as well as a free parameter \mathcal{R}_B (which is conventionally taken as unity). For $\mathcal{R}_\nu > 1$ (in which case we see a rising lightcurve before $t_{p,r}$), we have

$$\hat{\gamma} = \left(\frac{\mathcal{R}_t^{(\alpha-1)} \mathcal{R}_B^{(2\alpha+1)/3}}{\mathcal{R}_F} \right)^{\frac{3}{4\alpha-7}}, \quad \mathcal{R}_\nu = \left(\frac{\mathcal{R}_t^{3/2} \mathcal{R}_B^3}{\mathcal{R}_F^2} \right)^{\frac{3}{4\alpha-7}}, \quad (13)$$

and for $\mathcal{R}_\nu < 1$ (in which case we see a $\propto t^{-1/2}$ decaying lightcurve before $t_{p,r}$), we have

$$\hat{\gamma} = \mathcal{R}_t^{3/4} \mathcal{R}_B^{1/2}, \quad \mathcal{R}_\nu = \left(\frac{\mathcal{R}_t^{3/2} \mathcal{R}_B^3}{\mathcal{R}_F^2} \right)^{-3/4}. \quad (14)$$

Finally, the initial Lorentz factor γ_0 could be determined from $\hat{\gamma}$ through

$$\gamma_0 = \begin{cases} \hat{\gamma}, & \text{thin shell} \\ \gamma_c^2 / \hat{\gamma}, & \text{thick shell} \end{cases} \quad (15)$$

As we have commented before, in an idealized observational campaign, γ_c is essentially a known parameter (derived from E , n , T , z , etc.). Therefore, in an idealized data set, two γ_0 values could be measured (except for an unknown parameter \mathcal{R}_B usually of order unity) which correspond to the thin and thick shell cases, respectively. When t_\times is measured, $T \sim t_\times$ corresponds to the thick shell case, while $T < t_\times$ corresponds to the thin shell case.

In reality, due to delay of telescope response, the reverse shock peak time might not be caught definitely (e.g. the case for GRB 021004 and GRB 021211). In any case, one can always define a “pseudo reverse shock peak” by recording the very first data point in the observed $\propto t^{-2}$ lightcurve. Denoting this point as $(\bar{t}_{p,r}, \bar{F}_{\nu,p,r})$, one can similarly define

$$\bar{\mathcal{R}}_t \equiv \frac{t_{p,f}}{\bar{t}_{p,r}} \leq \mathcal{R}_t, \quad \bar{\mathcal{R}}_F \equiv \frac{\bar{F}_{\nu,p,r}}{F_{\nu,p,f}} \leq \mathcal{R}_F. \quad (16)$$

Repeat the above procedure, one can derive $\bar{\hat{\gamma}}$ and $\bar{\mathcal{R}}_\nu$ using (13) and (14), respectively, but with parameters \mathcal{R}_t , \mathcal{R}_F , $\hat{\gamma}$ and \mathcal{R}_ν substituted by their “bar” counterparts. The $\hat{\gamma}$ and $\bar{\mathcal{R}}_\nu$ values, however, are only upper (or lower) limits for $\hat{\gamma}$ and \mathcal{R}_ν for $\mathcal{R}_\nu > 1$ (or $\mathcal{R}_\nu < 1$). Usually we may be able to estimate $t_{p,r}$, and hence \mathcal{R}_t , from other constraints (e.g. $t_{p,r}$ has to be larger than T , etc.). In such cases, we can derive $\hat{\gamma}$ and \mathcal{R}_ν from $\bar{\hat{\gamma}}$ and $\bar{\mathcal{R}}_\nu$ with some correction factors involving $(\bar{\mathcal{R}}_t / \mathcal{R}_t)$. Using eqs. (10),

(11), (12), (16), and noticing $\bar{\mathcal{R}}_F / \mathcal{R}_F = (\bar{\mathcal{R}}_t / \mathcal{R}_t)^\alpha$ (as derived from $F_{\nu,r} \propto t^{-\alpha}$), we have $\hat{\gamma} = \bar{\hat{\gamma}} (\bar{\mathcal{R}}_t / \mathcal{R}_t)^{3/(4\alpha-7)}$, $\mathcal{R}_\nu = \bar{\mathcal{R}}_\nu (\bar{\mathcal{R}}_t / \mathcal{R}_t)^{3(4\alpha-3)/2(4\alpha-7)}$ for $\mathcal{R}_\nu > 1$; and $\hat{\gamma} = \bar{\hat{\gamma}} (\mathcal{R}_t / \bar{\mathcal{R}}_t)^{3/4}$, $\mathcal{R}_\nu = \bar{\mathcal{R}}_\nu (\mathcal{R}_t / \bar{\mathcal{R}}_t)^{(12\alpha-9)/8}$ for $\mathcal{R}_\nu < 1$. With estimated $\hat{\gamma}$, one can again derive γ_0 using (15). Notice that without catching $t_{p,r}$, both solutions for $\mathcal{R}_\nu > 1$ and $\mathcal{R}_\nu < 1$ are possible and one needs additional information (e.g. peak time of the radio flare) to break the degeneracy.

There are two caveats about our method. First, it involves a value of \mathcal{R}_B (the reverse to forward comoving magnetic field ratio), so one cannot determine γ_0 without specifying \mathcal{R}_B . The usual standard assumption is that $\mathcal{R}_B = 1$, but it may be larger since the central engine might be strongly magnetized. We note that there is another independent way to constrain γ_0 . Generally if t_\times could be measured one can directly derive (Sari & Piran 1999b)

$$\gamma_0 \geq \gamma_\times = \gamma_c (T/t_\times)^{3/8}, \quad (17)$$

which gives the value (or a lower limit) of γ_0 for the thin or thick shell case, respectively. This is the case for GRB 990123. When such independent information about γ_0 is available, constraints on \mathcal{R}_B may be obtained (see §5 for discussion of GRB 990123). Second, the radiative loss correction in the early forward shock evolution may be significant. This gives a correction factor of $\sim (t_{p,f}/t_\times)^{(17/16)\epsilon_e}$ (Sari 1997) to $F_{\nu,p,f}$. Strictly speaking, this should be taken into account when doing case studies.

4. CLASSIFICATION OF EARLY OPTICAL AFTERGLOWS

Regardless of the variety of early lightcurves, the reverse shock $F_{\nu,r} \propto t^{-2}$ emission component is expected to eventually join with the forward shock emission lightcurve. We can identify two cases (Fig.1). *Type I (Rebrightening)*: The reverse shock component meets the forward shock component before the forward shock peak time, as might have been observed in GRB 021004 (KZ03). *Type II (Flattening)*: The reverse shock component meets the forward shock component after the forward shock peak time. GRB 021211 may be a marginal such case (Fox et al. 2003; Li et al. 2003; Wei 2003).

The condition for a flattening type is $F_{\nu,r}(t_{p,f}) > F_{\nu,p,f}$. Using eqs.(11) and (12), noticing $F_{\nu,r} \propto t^{-\alpha}$, the flattening or type-II condition turns out to be

$$\hat{\gamma} < \mathcal{R}_B^{\frac{2\alpha+3}{4\alpha-3}} \mathcal{R}_\nu^{\frac{2}{4\alpha-3}} \quad (18)$$

for both $\mathcal{R}_\nu > 1$ and $\mathcal{R}_\nu < 1$. We can see that the type II condition is very stringent, especially when \mathcal{R}_B is not much above unity. We expect that rebrightening lightcurves should be the common situation. When a flattening lightcurve is observed, most likely one has $\mathcal{R}_\nu \gg 1$, i.e. the peak frequency for the reverse shock emission is well below the optical band. This should usually involve very low luminosities in both the reverse and forward shock emission. This might be the case of GRB 021211, which could have been categorized as an “optically dark” burst if the early reverse shock emission had not been caught. Alternatively, a flattening case may be associated with a strongly magnetized central engine, since a higher \mathcal{R}_B can significantly ease the type II condition.

5. CASE STUDIES

Early optical afterglows have been detected from GRB 990123, GRB 021004 and GRB 021211. Unfortunately, none of these observations give us an “idealized” data set, i.e., in none of these cases both “peaks” are identified. Our method therefore could not be applied straightforwardly. Nonetheless, we can use the correction factors mentioned in §3 to estimate γ_0 in these cases. We expect that *Swift* will provide the ideal data set for more bursts on which our method could be utilized directly.

1. GRB 990123: The basic parameters of this burst include² (e.g. Kobayashi & Sari 2000 and references therein) $E_{52} \sim 140$, $z = 1.6$, $T_2 \sim 0.6$, $\alpha \sim 2$. This gives $\gamma_c \sim 305n^{-1/8}$ (notice weak dependence on n). The reverse shock peak was well determined: $(t_{p,r}, F_{\nu,p,r}) \sim (50\text{s}, 1\text{Jy})$. The lightcurve shows $\mathcal{R}_\nu > 1$. Since the early rising lightcurve is caught, t_x is directly measured, i.e., $t_x \sim t_{p,r} \sim T$. This is a marginal case, and $\gamma_0 \sim \gamma_c \sim 300n^{-1/8}$ (eq.[17]). Unfortunately, the forward shock peak was not caught. Assuming $t_{p,f} \sim 0.1$ d, one has $\mathcal{R}_t \sim 170$, and $\mathcal{R}_F \sim 5000$. The radiative correction factor is ~ 2 by adopting $\epsilon_e \sim 0.13$ (Panaitescu & Kumar 2001). With this correction, one has $\hat{\gamma} \sim (0.07\mathcal{R}_B^{5/3})^3$ (eq.[13]). By requiring $\hat{\gamma} \sim 300n^{-1/8}$, $\mathcal{R}_B \sim 15n^{-1/40}$ is required. We conclude that GRB 990123 is giving us the first evidence for a strongly magnetized central engine.

2. GRB 021004: The parameters of this burst are (e.g. KZ03 and references therein) $E_{52} \sim 5.6$, $z = 2.3$, $T_2 \sim 1$. We have $\gamma_c \sim 190n^{-1/8}$. The forward shock peak is reasonably well measured, but the reverse shock peak is not caught. Using the first data point as modeled in KZ03, we have $\mathcal{R}_t \sim 12$, $\mathcal{R}_F \sim 2$. Solving for $\hat{\gamma}$ and \mathcal{R}_ν , we get $\hat{\gamma}_0 \leq 220\mathcal{R}_B^5$ for $\mathcal{R}_\nu > 1$ and $\alpha \sim 2$ (in the asymptotic phase), and $\hat{\gamma} \geq 6.5\mathcal{R}_B^{1/2}$ for $\mathcal{R}_\nu < 1$. The detailed modeling of the lightcurve suggests $\mathcal{R}_\nu > 1$ and thin shell, so that $\gamma_0 \sim 120$ for $\mathcal{R}_B \sim 1$ (KZ03).

3. GRB 021211: The basic parameters of this burst include $E_{52} \sim 0.6$, $z = 1.0$, $T_2 \sim 0.15$, $\alpha \sim 1.8$ (Li et al. 2003; Fox et al. 2003; and references therein), so that

$\gamma_c \sim 240n^{-1/8}$. Neither the forward nor the reverse shock peaks are identified. Assuming that the forward shock peak occurs close to the flattening break (marginal type-II flattening case) and taking the first data point of the early lightcurve, we get $\mathcal{R}_t \sim 20$, $\mathcal{R}_F \sim 30$. Since $\mathcal{R}_\nu < 1$ is unlikely for a flattening (type-II) lightcurve (eq.[18]), we get $\hat{\gamma} \leq (0.4\mathcal{R}_B^{1.5})^{15}$ with $\mathcal{R}_\nu > 1$. For any reasonable $\hat{\gamma}$, \mathcal{R}_B has to be somewhat larger than unity. Other information is needed to estimate $\hat{\gamma}$ and γ_0 .

6. CONCLUSIONS AND IMPLICATIONS

We have discussed a clean recipe for constraining the initial Lorentz factor γ_0 of GRB fireballs by making use of the early optical afterglow data alone. Data in other bands (e.g. X-ray or radio) are usually not needed. The input parameters are ratios of observed emission quantities, so that poorly known model parameters related to the shock microphysics (e.g. ϵ_e , ϵ_B , etc.) largely cancel out. This approach is readily applicable in the *Swift* era when many early optical afterglows are expected to be regularly caught. By combining it with other information, this method may provide, for the first time, information about the magnetic content of the ejecta. Such information about the fireball initial Lorentz factor and about whether the central engine is strongly magnetized are helpful for the identification of the GRB prompt emission site and mechanism, which are currently uncertain (e.g. Zhang & Mészáros 2002).

We have also classified the early optical afterglow lightcurves into two types. The rebrightening case (type-I) should be very common. The flattening case (type-II) is rare, and when detected, is likely to involve a low luminosity or a strongly magnetized central engine. There is evidence that the central engine of GRB 990123 is strongly magnetized.

This work is supported by NASA NAG5-9192, NAG5-9153 and the Pennsylvania State University Center for Gravitational Wave Physics, which is funded by NSF under cooperative agreement PHY 01-14375.

REFERENCES

Akerlof, C. W. et al. 1999, *Nature*, 398, 400
 Crew, G. et al. 2002, GCN 1734, (<http://gcn.gsfc.nasa.gov/gcn/gcn3/1734.gcn3>)
 Fan, Y. Z., Dai, Z. G., Huang, Y. F. & Lu, T. 2002, ChJAA, 2, 449
 Fox, D. W. 2002, GCN 1564 (<http://gcn.gsfc.nasa.gov/gcn/gcn3/1564.gcn3>)
 Fox, D. W. & Price, P. A. 2002, GCN 1731 (<http://gcn.gsfc.nasa.gov/gcn/gcn3/1731.gcn3>)
 Fox, D. W. et al. 2003, ApJ, 586, L5
 Kobayashi, S. 2000, ApJ, 545, 807 (K00)
 Kobayashi, S., Piran, T. & Sari, R. 1999, ApJ, 513, 669
 Kobayashi, S. & Sari, R. 2000, ApJ, 542, 819
 Kobayashi, S. & Zhang, B. 2003, ApJ, 582, L75 (KZ03)
 Li, W., et al., 2002, GCN 1737 (<http://gcn.gsfc.nasa.gov/gcn/gcn3/1737.gcn3>)
 Li, W., et al. 2003, ApJ, 586, L9
 Mészáros, P. & Rees, M. J. 1997a, ApJ, 476, 231
 —. 1997b, ApJ, 482, L29
 —. 1999, MNRAS, 306, L39
 Panaitescu, A., & Kumar, P. 2001, ApJ, 560, L49
 Park, H. S., Williams, G. & Barthelmy, S. 2002, GCN 1736 (<http://gcn.gsfc.nasa.gov/gcn/gcn3/1736.gcn3>)
 Sari, R. 1997, ApJ, 489, L37
 Sari, R. & Piran, T. 1995, ApJ, 455, L143
 —. 1999a, ApJ, 517, L109
 —. 1999b, ApJ, 520, 641
 Sari, R., Piran, T. & Narayan, R. 1998, ApJ, 497, L17
 Shirasaki, Y. et al. 2002, GCN 1565 (<http://gcn.gsfc.nasa.gov/gcn/gcn3/1565.gcn3>)
 Soderberg, A. M., & Ramirez-Ruiz, E. 2002, MNRAS, 330, L24
 Usov, V. V. 1992, *Nature*, 357, 472
 Wang, X. Y., Dai, Z. G., & Lu, T. 2000, MNRAS, 319, 1159
 Wei, D. M. 2003, A&A, in press (astro-ph/0301345)
 Wolzniak, P., et al. 2002, GCN 1757 (<http://gcn.gsfc.nasa.gov/gcn/gcn3/1757.gcn3>)
 Zhang, B. & Mészáros, P. 2002, ApJ, 581, 1236

²Hereafter we assume that the kinetic energy of the fireball in the deceleration phase is comparable to the energy released in gamma-rays in the prompt phase.

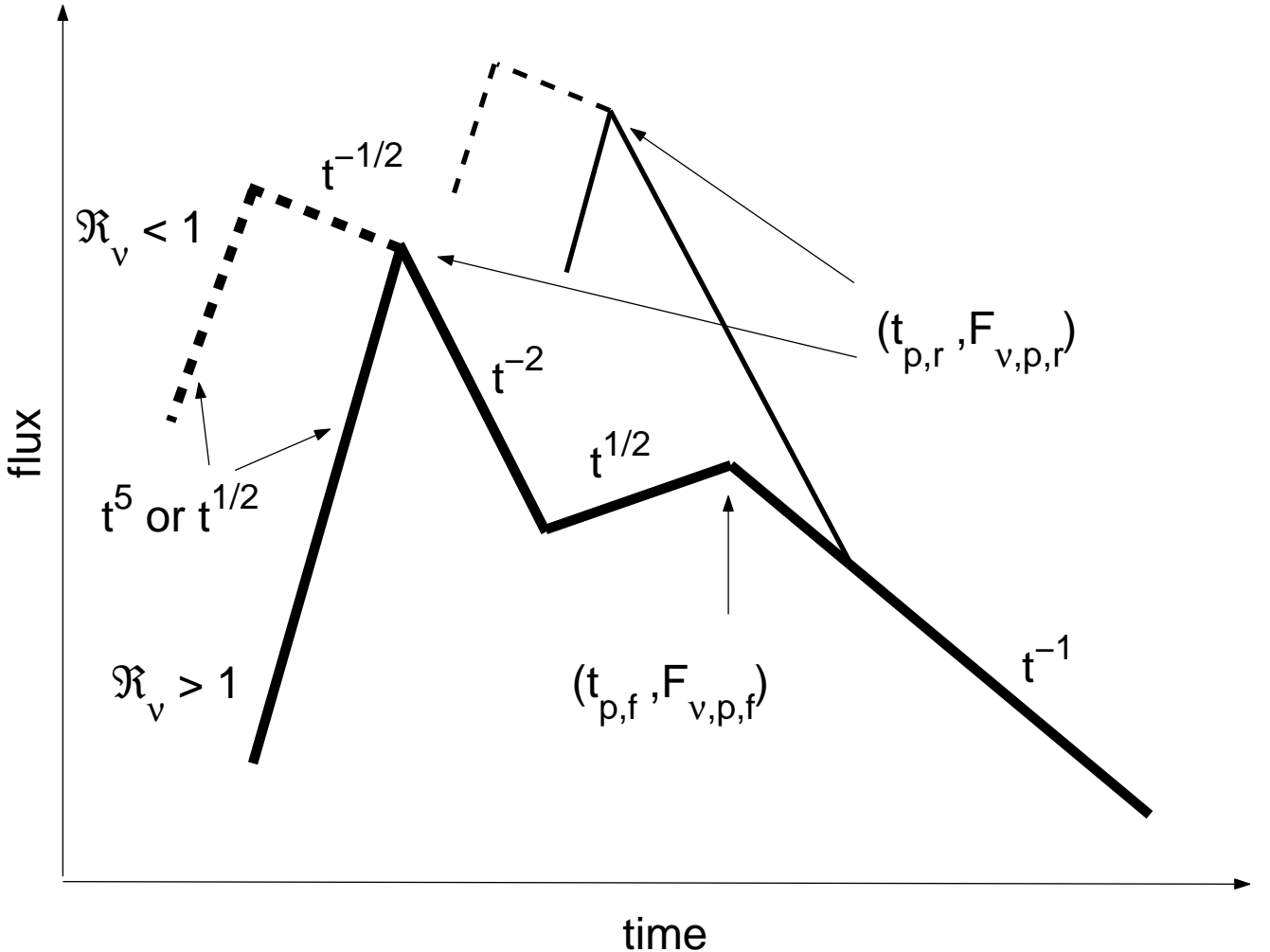


FIG. 1.— Typical lightcurves of the reverse-forward shock emission combinations. The thick lines depict a typical “rebrightening” (type I) lightcurve, while thin lines indicate a typical “flattening” (type II) lightcurve. The forward shock peak $(t_{p,f}, F_{v,m,p})$ is defined at the transition point of the $\propto t^{1/2}$ to $\propto t^{-1}$ lightcurves. The reverse shock peak $(t_{p,r}, F_{v,m,r})$ is defined at the beginning of the $\propto t^{-2}$ segment for the reverse shock emission. Before this point, the lightcurve is $\propto t^5$ (thin shell) or $\propto t^{1/2}$ (thick shell) for $\mathcal{R}_\nu \equiv \nu_R/\nu_{m,r}(t_\times) > 1$ (usually the case), and $\propto t^{-1/2}$ for $\mathcal{R}_\nu < 1$.